FABRICATION OF OPEN-CELL ALUMINA CERAMIC FOAMS VIA THE REPLICA METHOD

Berkay MENÇ

Gazi University, Faculty of Technology, Department of Metallurgical & Materials Engineering 06500, Beşevler, Ankara, Türkiye

ORCID**:** 0009-0004-2010-5720

Email: berkaymenc@gmail.com

Yusuf ÖZÇATALBAŞ

Gazi University, Faculty of Technology, Department of Metallurgical & Materials Engineering 06500, Beşevler, Ankara,Türkiye

ORCID: 0000-0002-4256-8492

Email:ozcatalbas@gazi.edu.tr

ABSTRACT

Metallic and ceramic foams are divided into two basic classes based on their pore structure: closed and open pore. Differences in cell structure are directly related to the manufacturing method and the parameters used. Open-pore foams, due to their large specific surface area, are preferred in heat exchangers. Ceramic foams, due to their high liquid/gas permeability and corrosion and high temperature resistance, are preferred in filtration and separation processes, and in water treatment applications where unwanted ions can be removed from solution. In this study, open-cell Al-based alumina ceramic foams with varying pore sizes were fabricated using the powder metallurgy method combined with aluminum powder and the polyurethane foam (PU) replication technique. The structure obtained after the removal of the PU at 500°C 3 hours was subsequently sintered in an open atmosphere for 6 hours at temperatures of 850°C, 900°C, and 950°C. X-Ray diffraction (XRD) analyses, scanning electron microscopy (SEM) and microstructural investigations were performed on the fabricated ceramic-coated foams. During the high-temperature oxidative sintering process conducted in an open atmosphere, alumina ceramic-coated foams with optimal properties were successfully obtained at 950 °C, achieved through the sintering mechanism resulting from the oxidation of the aluminum powders.

Keywords: Open-cell foam, Powder metallurgy, Metallic foam, Ceramic foam

INTRODUCTION

Advanced porous metallic and ceramic materials have played a critical role in industrial applications in recent years, owing to their unique combination of physical and thermal properties. Key advantages that distinguish these materials include characteristics such as high specific surface area, low density, chemical stability, and thermal shock resistance [1-3]. Ceramic foams, which are classified as open-cell or closed-cell based on their pore morphology, are primarily utilized in environments characterized by demanding conditions, such as molten metal filtration, catalyst support units, heat shields, and biomedical implants. [4-7]. In contrast to metallic foams, ceramic foams offer oxidation resistance and dimensional stability at elevated temperatures. Specifically, open-cell ceramic foams maximize heat and mass transfer by generating turbulent flow, owing to their interconnected pore networks that allow fluid permeability. [8]. Studies have focused on various ceramic materials such as silicon carbide (SiC), zirconia (ZrO_2), and alumina (Al_2O_3). Among these, alumina stands out for its high melting point, mechanical strength, and cost-effectiveness. [9]. Although various techniques such as "direct foaming" and "gel casting" are used in the production of ceramic foams, the polymer sponge replica method developed by Schwartzwalder and Somers is the most widely accepted technique on an industrial scale [10]. This method is based on the principle of impregnating a flexible polyurethane foam (PUF) with a ceramic slurry, removing the excess slurry, and subsequently sintering the ceramic structure by burning out the organic scaffold via applied thermal treatments. A representation of the structure obtained after the removal of the organic-based template material is provided in Figure 1.

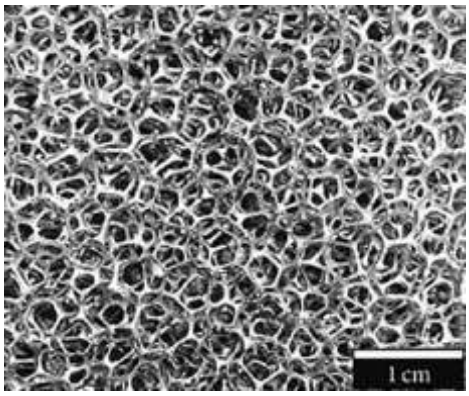


Figure 1. Open-cell metallic foam [11]

The biggest advantage of the method is that the pore structure of the starting polymer can be almost exactly copied into the final ceramic product. [12]. Recent studies have demonstrated that the fundamental challenge in ceramic foams fabricated via the replica method is optimizing the inverse correlation between mechanical strength and porosity. Betke et al. [13], investigated the influence of mixture composition on cellular alumina, while other researchers focused on the effect of the sintering temperature on microstructural defects [14]. However, while the effect of the sintering temperature on the microstructural evolution during the production of alumina-based ceramic foams is known, studies focusing specifically on the liquid phase mechanisms formed within the matrix during the sintering process and the interaction of this phase with the alumina grains are limited. The presence of the liquid phase has a significant role on the densification behavior and grain growth of the ceramic skeleton, and a detailed understanding of this mechanism is needed. [15-18]. The objective of this study is to investigate the physical changes and microstructural characteristics of open-cell pure aluminum-based alumina (Al2O3) coated ceramic foams, fabricated via the replica method using pure aluminum powder and polyurethane (PU) sponges, with respect to different sintering temperatures.

MATERIAL AND METHOD

2.1. Materials

In the experiments, pure Al powders with 99.9 % purity and a particle size of < 10 µm were utilized. Polyurethane (PU) sponges ($C_{25}H_{42}N_2O_6$) with pore sizes of 10, 20 ve 30 ppi (pores per inch) were selected as the organic template material. Polyvinyl alcohol (PVA) in powder form was used as the binder, and deionized water was employed as the solvent.

2.2. Sample Preparition and Process

The production process of the alumina-coated foams comprises the following stages: slurry mixture preparation, template material impregnation, drying, binder and template material removal, and sintering. During the fabrication of the specimens, the procedure followed the process flow chart presented in Figure 2.

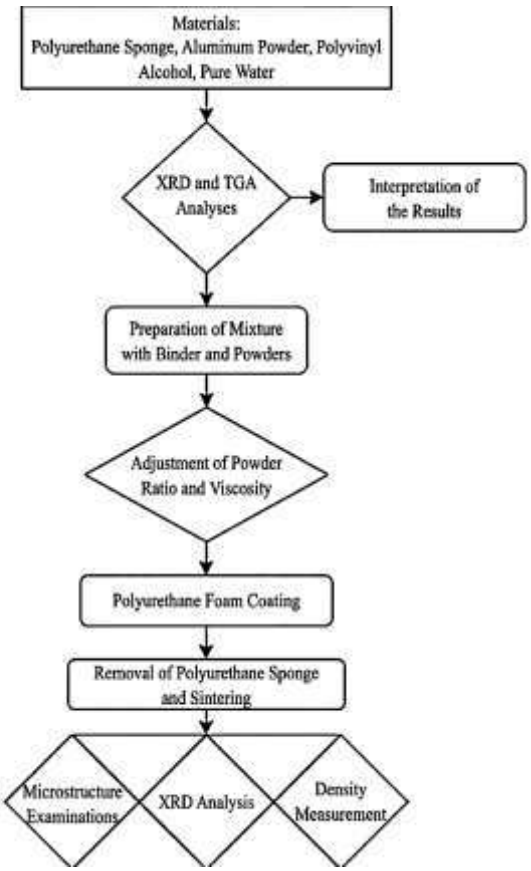


Figure 2. Process flowchart in production

Firstly, a slurry mixture was prepared by mixing deionized water and PVA using a turbula mixer, and the mixture was subsequently allowed to settle for 1 day. Moreover, pure Al powders at a 70% powder ratio determined to be optimal for viscosity, were introduced into this solution, resulting in a mechanically homogeneous slurry. PU sponges with pore sizes of 10 ppi, 20 ppi, and 30 ppi were cut into 20x20x20 mm dimensions using a foam cutting device. The cut sponges were then immersed in the prepared mixture to ensure homogeneous coating. The coated samples were first stored at room temperature for 1 day.

The dried specimens were processed in a furnace under ambient atmospheric conditions for the removal of the binder and template material. Initially, the PVA (binder) was eliminated from the structure at 350°C for 3 hours. Subsequently, the template material (PUF) was removed from the structure by holding the specimens at 500°C for 3 hours. After the template material was removed for the sintering process, the remaining aluminum powders were sintered together at different temperatures (850 °C, 900 °C and 950 °C) under normal atmospheric conditions.

Figure 3 shows the production phase of the samples and Figure 4 depicts the image of the alumina coated metallic foams after the sintering process.

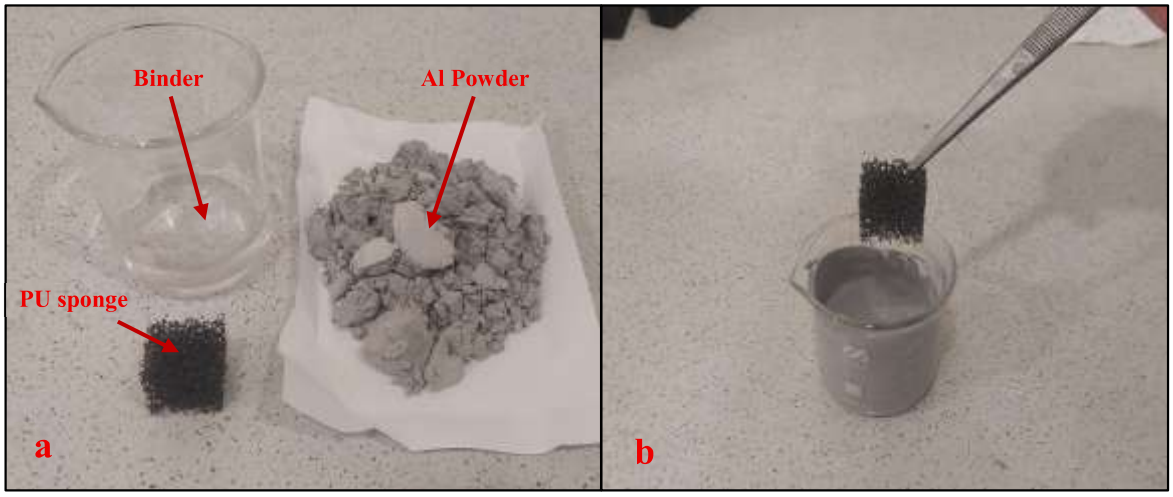


Figure 3. a) Materials which is used when studies **b)** Process for coating the template material with the prepared aluminum slurry.

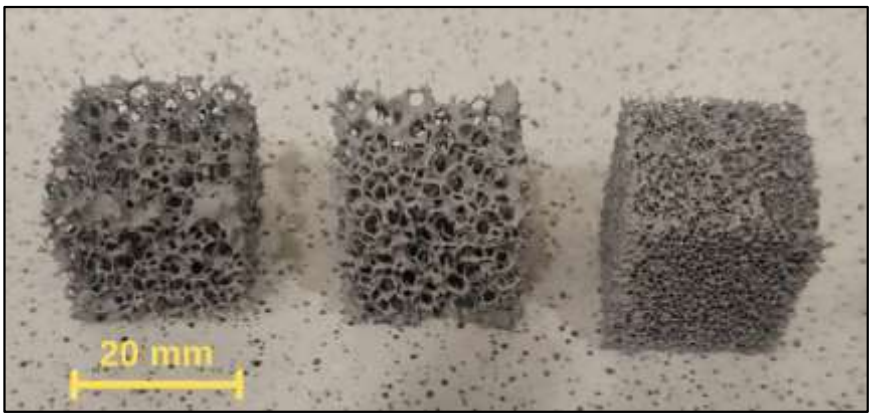


Figure 4. Sintered Al based Al_2O_3 coated foams

5. EXPERIMENTAL RESULTS

Scanning electron microscopy (SEM) analysis of the ceramic foams sintered under open atmospheric conditions was conducted using a JEOL JSM 6060 LV instrument, with the objective of investigating the sintering effects and the morphology of the resulting foam. The SEM micrographs focused on the 20 ppi foam material sintered at 950 °C. As observed in Figure 5a, after the removal of the PU template material, the aluminum powders successfully replicated the shape of the template, effectively forming the cell walls and columns. A micrograph of the fractured surface of the produced foam is presented in Figure 5b. Independent spherical structures formed in various regions on the cell walls are noteworthy (indicated by arrows in Figure 5b). One of these structures is shown at higher magnification in Figure 5c. The Al powders introduced into the structure during the production process are <10 µm in size, which is observable in Figure 5d. The size of these coarse spherical structures formed on the cell walls typically ranges from 50 to 100 µm.

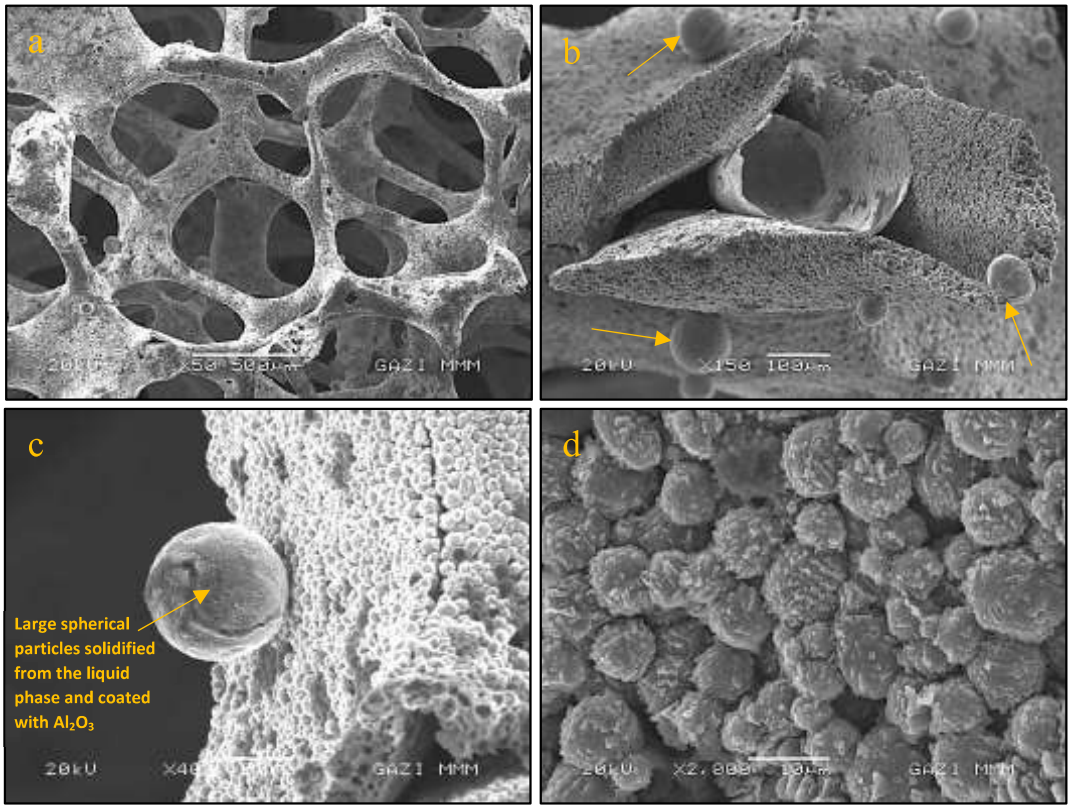


Figure 5. SEM micrographs of the alumina foam sintered at 950°C at different magnifications: **a)** general view, **b)** viewed across the fractured surface, **c)** Solid Al grown in liquid form and coated with alumina and **d)** Initial size alumina coated Al particles

During high-temperature sintering in an open atmosphere, the liquid phase formed in certain sections of the cell walls was observed to migrate towards the surface via capillary action, subsequently forming and solidifying into a spherical shape. The stability of the foam structure, which did not fully transition into the liquid phase or collapse despite the high sintering temperature (950 °C), can be attributed to the rapid and excessive oxidation of the Al particles in the open atmosphere sintering environment, which resulted in the formation of an alumina (Al_2O_3) layer on the powder surfaces. The angular pointed structures clearly visible on the surface of Al powder particles in Figure 5d are oxide structures formed under open atmospheric conditions during the sintering process.

The spherical structures formed in the produced samples were identified as containing dense Al_2O_3, as determined by the XRD analysis given in Figure 6. Generally, peak intensities indicate that the alumina content on Al surfaces increases with increasing sintering temperature. However, the highest alumina content is observed in the XRD analysis of foam sintered at 900°C. This may be attributed to the increased oxidation rate of the sinter medium by leaving the furnace door partially open for a certain period of time. This condition enhances the formation of Al_2O_3 on the surface of the Al powders within the furnace atmosphere.

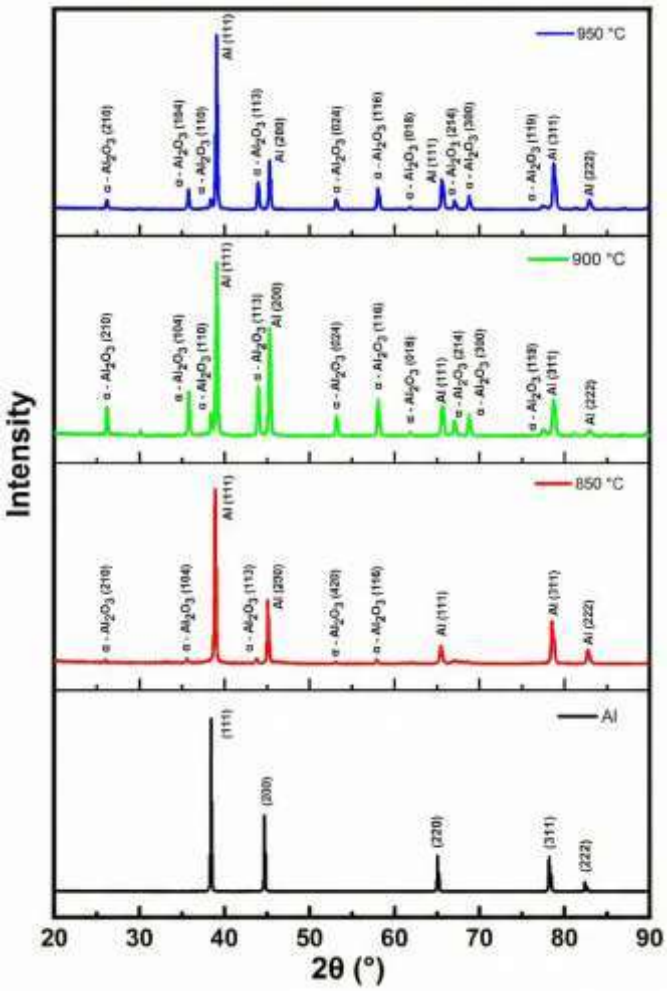


Figure 6. XRD analysis result of pure Al and foams sintered in open atmosphere

6. REFERENCES

1) Ohji, T., & Fukushima, M. (2022). Macro-porous ceramics: processing and properties. International Materials Reviews, 67(1), 1-28.

2) Türker, M. (2025) Production of Al-based Foam Using Powder Metallurgy method, Its Application Areas and Use for Energy Absorption in Polymer-based Armors. *Gazi Üniversitesi Fen Bilimleri Dergisi Part C: Tasarım ve Teknoloji*, *13*(4).

3) Turker, M., Ozcatalbas, Y., Cinici, H., Gokmen, U., & Uzun, A. (2011, March). Effect of Foaming Agent on The Structure and Morphology of Al and Alumix 231 Foams Produced by Powder Metallurgy. In Materials Science Forum (Vol. 672, pp. 297-302). Trans Tech Publications Ltd.

4) Dammler, K., Schelm, K., Betke, U., Fey, T., & Scheffler, M. (2021). Open-cellular alumina foams with hierarchical strut porosity by ice templating: A thickening agent study. *Materials*, *14*(5), 1060.

5) Chakraborty, S., O'Malley, R. J., Bartlett, L., & Xu, M. (2018). Efficiency of solid inclusion removal from the steel melt by ceramic foam filter: Design and experimental validation.

6) Menç, B., & Özçatalbaş, Y. (2026). Manufacturing and characterization of open-cell aluminum foam by powder metallurgy. Materials Science and Technology, 42(1), 93-105

7) Baino, F., Novajra, G., & Vitale-Brovarone, C. (2015). Bioceramics and scaffolds: a winning combination for tissue engineering. *Frontiers in bioengineering and biotechnology*, *3*, 202.

8) Bianco, N., Contento, G., Cunsolo, S., Iasiello, M., Naso, V., & Oliviero, M. (2017). Heat transfer enhancement in open-cell foams. *Annual review of heat transfer*, *20*.

9) Gonzenbach, U. T., Studart, A. R., Tervoort, E., & Gauckler, L. J. (2007). Macroporous ceramics from particle-stabilized wet foams. *Journal of the American Ceramic Society*, *90*(1), 16-22.

10) Karl, S., & Somers, A. V. (1963). *U.S. Patent No. 3,090,094*. Washington, DC: U.S. Patent and Trademark Office.

11) Wan, T., Liu, Y., Zhou, C., Chen, X., & Li, Y. (2021). Fabrication, properties, and applications of open-cell aluminum foams: A review. *Journal of Materials Science & Technology*, *62*, 11-24.

12) Studart, A. R., Gonzenbach, U. T., Tervoort, E., & Gauckler, L. J. (2006). Processing routes to macroporous ceramics: a review. *Journal of the American Ceramic Society*, *89*(6), 1771-1789.

13) Betke, U., Dalicho, S., Rannabauer, S., Lieb, A., Scheffler, F., & Scheffler, M. (2017). Impact of slurry composition on properties of cellular alumina: A computed tomographic study. *Advanced Engineering Materials*, *19*(10), 1700138.

14) Betke, U., Mendoza, D. C., & Scheffler, M. (2023). Reticulated open-cellular aluminum nitride ceramic foams: Effect of sintering aids on microstructural, thermal, and mechanical properties. *International Journal of Applied Ceramic Technology*, *20*(1), 204-212.

15) Chen, J., Liang, X., Li, Y., Wu, Z., Wang, Q., Pan, L., & Sang, S. (2025). Preparation and properties of alumina reticulated porous ceramics for high-temperature porous medium combustion. *Ceramics International*.

16) German, R. M., Suri, P., & Park, S. J. (2009). Liquid phase sintering. *Journal of materials science*, *44*(1), 1-39.

17) Zu, Y., Chen, G., Fu, X., Luo, K., Wang, C., Song, S., & Zhou, W. (2014). Effects of liquid phases on densification of TiO2-doped Al2O3–ZrO2 composite ceramics. *Ceramics International*, *40*(3), 3989-3993.

18) Jiao, R., Rong, S., & Wang, D. (2022). Effect of dual liquid phase sintering aids on the densification and microstructure of low temperature sintered alumina ceramics. *Ceramics International*, *48*(5), 6138-6147.